

Rapid 3D fMRI of the Hemodynamic Response Function

Martin A. Lindquist¹, Cun-Hui Zhang², Gary Glover³ and Lawrence Shepp²

¹Department of Statistics, Columbia University

²Department of Statistics, Rutgers University

³Department of Radiology, Stanford University



THE STATE UNIVERSITY OF NEW JERSEY
RUTGERS
Department of Statistics

INTRODUCTION

We introduce a new approach towards the acquisition and analysis of fMRI data that allows one to perform rapid 3D fMRI studies with a temporal resolution of 100ms.

The high temporal resolution allows for

- Effective modeling of periodic nuisance parameters (e.g. heart rate and respiration).
- Accurate estimates of latency differences across the brain. In particular our method appears sensitive to the initial negative dip and allows for estimation of its relative timing across regions.

Our acquisition strategy is based on repeatedly sampling a small central region of 3D k-space every 100ms using an echo-volumar imaging trajectory (Fig. 1).

The feasibility and efficiency of the approach is confirmed using data from a visual-motor and an auditory-motor-visual task.

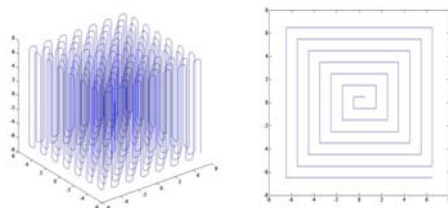


Figure 1. (A) An implementation of the Echo-Volumar Imaging trajectory. (B) The trajectory shown in (A) projected onto the xy-plane.

METHODS

Data Acquisition

Our approach involves sampling the central portion of 3D k-space in a single-shot during a 100ms time window. Our sampling trajectory travels through k-space with the goal of hitting each coordinate on a 3D Cartesian grid. It starts at the point $(0,0,z_{min})$ and moves along the z-axis to the point $(0,0,z_{max})$. Upon reaching this point the trajectory makes a half circular loop over to the point $(1,0,z_{max})$ and then continues along the z-axis in the opposite direction until it reaches $(1,0,z_{min})$. The trajectory continues in a similar manner until it has completed a square spiral in the xy-plane. To ensure that each straight line consists of the same number of points, each line begins at the same speed u , accelerates in the first half of the line and de-accelerates in the second half. The trajectory then travels in a half circle with constant speed u before starting the process again on the next line. Using this approach it is possible to sample the central portion of 3D k-space with dimensions $14 \times 14 \times 14$ in the allocated time window (Fig. 1).

Image Reconstruction

The data is sampled on a Cartesian grid in the xy-plane, and linear interpolation can be used to obtain uniformly spaced measurements in the z-direction. After interpolation, the k-space data consists of 2,744 (e.g. $14 \times 14 \times 14$) uniformly sampled measurements in 3D k-space, and reconstruction is performed using the fast Fourier transform (FFT). Prior to reconstruction the data is zero-filled to a resolution of $64 \times 64 \times 64$, and a prolate spheroidal wave function filter is applied to reduce truncation artifacts.

Statistical Analysis

After reconstruction, statistical analysis is conducted voxel-wise using the following three step procedure:

1. A standard GLM analysis is performed to detect regions which exhibit a significant positive BOLD signal.
2. Time courses from active voxels are decomposed into trend, task and periodic components (Fig. 2). Due to the high time resolution, the periodic signal induced by heart beat and respiration is contained in separate frequencies from task-related signal and can be effectively filtered out.
3. Bootstrap distributions are calculated for the amplitude of the negative dip, as well as for the time it takes for the dip to reach its peak (time-to-dip). Using these distributions we can perform statistical tests to:
 - (a) detect voxels with significant negative dipoles.
 - (b) compare the time-to-dip across regions.

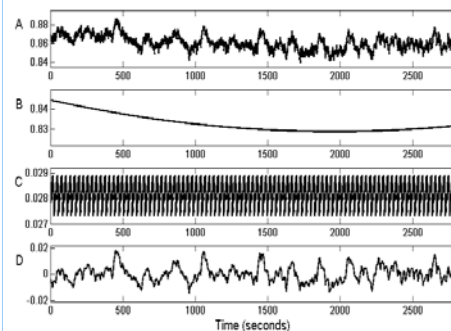


Figure 2. (A) A typical time course decomposed into (B) quadratic drift, (C) seasonal nuisance parameters and (D) task related signal. The length of the period for the nuisance parameters is approximately 3 seconds and represents artifacts due to respiration.

Experiment I

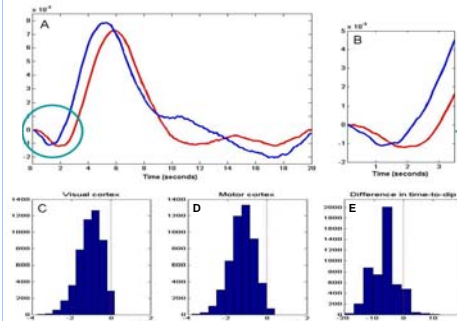


Figure 3. (A) Time courses from the visual (blue) and motor (red) cortices averaged over the 14 repetitions of the visual-motor stimulus. (B) The first 3 seconds following stimulation for the two time courses appearing in A. The dip appears earlier in the visual cortex than the motor cortex, which is consistent with the experimental paradigm. (C-E) The results of bootstrap tests show a significant dip in the visual (C) and motor (D) cortices, as well as a significant difference in time-to-dip between the cortices (E).

Experiment II

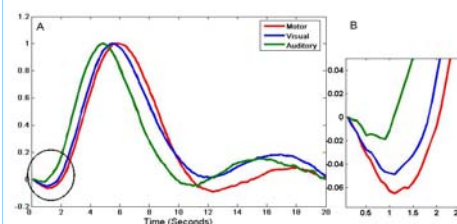


Figure 4. (A) Time courses from the auditory (green), visual (blue) and motor (red) cortices averaged over the 14 cycles. (B) The first 3 seconds following stimulation for the three time courses.

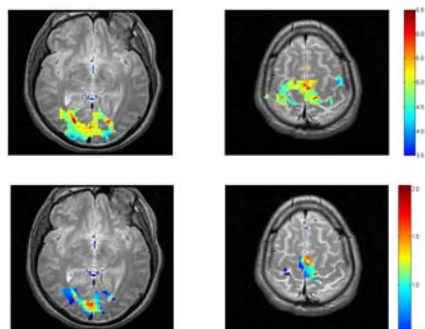


Figure 5. (Top row) Maps of the time-to-rise in voxels with significant activation for two slices in Experiment II. A slice containing the visual cortex is shown to the left and one showing the motor cortex to the right. The results indicate that the rise peaks earlier in the visual than the motor cortex. (Bottom row) Maps of the time-to-dip in voxels with significant negative dipoles in the same two slices. The dip peaks earlier in the visual than the motor cortex indicating that important latency information is present in the dip.

Experimental Design

Two high temporal resolution fMRI experiments were performed to confirm the feasibility and efficiency of our approach.

Experiment I: The first paradigm consisted of fifteen cycles of 20s intervals. At the beginning of each interval a 100ms light flash was presented. The subject was instructed to press a button immediately after sensing the flash, thereby leading to activation of the motor cortex. During each 20 second interval, images were acquired every 100ms.

Experiment II: The second paradigm also consisted of fifteen cycles of 20s intervals. At the beginning of each interval a tone was sounded through the subject's headphones. The subject was instructed to press a button immediately after hearing the tone. Upon pressing the button a 100ms light flash was presented, leading to activation of the visual cortex. During each 20 second interval, images were acquired every 100ms.

A healthy male volunteer participated in the study after giving informed consent. The data was acquired with an effective TE 30ms, flip angle 20 degrees, field of view 200mm, slice thickness 185mm and bandwidth 250kHz. The experiment was performed on a 3.0T whole body scanner (General Electric Medical Systems, Milwaukee, WI, USA).

In both experiments the first cycle was thrown out and the data consisted of 14 cycles with a total of 2800 time points. The resulting k-space data was reconstructed and statistical analysis was performed as outlined above.

RESULTS

Statistical analysis was performed using the GLM approach and voxels with significant activation were identified ($p < 0.005$). Fig. 3A shows time courses extracted from the center of the visual and motor cortices, respectively, for Experiment I. Fig. 3B shows the first 3 seconds following activation. Clear negative dips appear in both the visual and motor cortex. Bootstrap tests (Figs. 3C-E) show that while both dips are statistically significant, the dip in the visual cortex occurs earlier than in the motor cortex.

Fig. 4 shows similar results for Experiment II. We see that there is a significant dip in the auditory cortex followed by dips in the visual and motor cortices. This corresponds to what is expected by the experimental paradigm. Interestingly, if we instead use the positive BOLD response to infer the timing of activation, the order between the visual and motor cortices is confounded indicating that the vascular response is faster in the visual than the motor cortex. This can also be seen in Fig. 5 which shows maps over both the time-to-peak positive BOLD response, as well as the time-to-peak dip.

CONCLUSIONS

- We introduce a new imaging technique that sacrifices spatial for temporal resolution.
- Parallel imaging techniques can be used to reclaim some of the lost spatial resolution (future research).
- The high temporal resolution of our method allows one to effectively study the hemodynamic response function. Statistical analysis can be performed solely on the negative dip.
- It also allows for accurate estimation of the heart beat and respiration without aliasing.

REFERENCES

- Lindquist, M.A. Zhang, C.-H., Glover, G. and Shepp, L. (2007). Acquisition and Statistical Analysis of Rapid 3D fMRI data. *In submission*.
- Lindquist, M.A. Zhang, C.-H., Glover, G. and Shepp, L. (2006). Rapid Three-Dimensional Functional Magnetic Resonance Imaging of the Negative BOLD Response. *In submission*.
- Lindquist, M.A. Zhang, C.-H., Glover, G., Shepp, L. and Yang, Q. (2006). A Generalization of the Two Dimensional Prolate Spheroidal Wave Function Method for Non-Rectilinear MRI Data Acquisition Methods. *IEEE Transactions in Image Processing*, 15(9), 2792-2804.